

TBA

TBA

Nucleon strange electromagnetic form factors

Jeremy Green

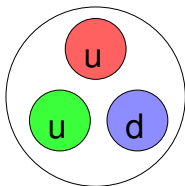
Institut für Kernphysik, Johannes Gutenberg-Universität Mainz

Fundamental Parameters from Lattice QCD
Mainz Institute for Theoretical Physics
August 31–September 11, 2015

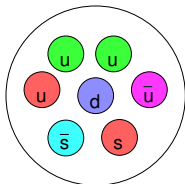
- 1 Introduction
- 2 Results from experiment
- 3 Lattice QCD methodology
- 4 Numerical results

Nucleons

The *net* quark content of a proton is uud and of a neutron is ddu .



But quantum fluctuations can produce gluons and $\bar{q}q$ pairs, including also heavier quarks (s, \dots).



Electromagnetic form factors

We can probe the structure of a proton using virtual photons, which couple to quarks via the current

$$J_\mu^Y = \frac{2}{3} \bar{u} \gamma_\mu u - \frac{1}{3} \bar{d} \gamma_\mu d - \frac{1}{3} \bar{s} \gamma_\mu s + \dots$$

Symmetries constrain matrix elements between proton states with momenta p and p' :

$$\langle p' | J_\mu^Y | p \rangle = \bar{u}(p') \left[\gamma_\mu F_1^Y(Q^2) + \frac{i \sigma_{\mu\nu} (p' - p)^\nu}{2m_p} F_2^Y(Q^2) \right] u(p),$$

where $Q^2 = -(p' - p)^2$ is the four-momentum transfer and $F_{1,2}^Y$ are the Dirac and Pauli form factors.

Electric and magnetic form factors:

$$G_E^Y(Q^2) = F_1^Y(Q^2) - \frac{Q^2}{(2m_p)^2} F_2^Y(Q^2), \quad G_M^Y(Q^2) = F_1^Y(Q^2) + F_2^Y(Q^2)$$

Electromagnetic form factors

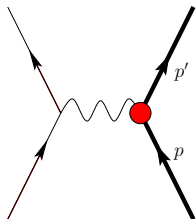
In the *nonrelativistic limit*, $G_E(Q^2)$ and $G_M(Q^2)$ are Fourier transforms of the charge and magnetization densities in a proton.

- ▶ $G_E^y(0) = 1$, the charge of a proton
- ▶ $G_M^y(0) = \mu$, the magnetic moment of a proton, in units of the nuclear magneton $\mu_N = \frac{e}{2m_p}$

Even though this interpretation doesn't hold relativistically, it is still used to *define* the charge and magnetic radii using the derivatives at $Q^2 = 0$:

- ▶ $r_E^2 = -6G_E^{y'}(0)$
- ▶ $r_M^2 = -6G_M^{y'}(0)/\mu$

Elastic ep scattering



Elastic scattering of an electron off a fixed proton target has a leading contribution from single photon exchange,

which contributes to the cross section

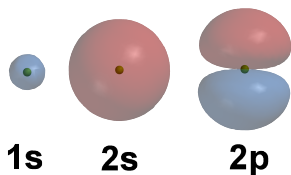
$$\sigma \propto G_E^Y(Q^2)^2 + \frac{\tau}{\epsilon} G_M^Y(Q^2)^2, \quad \tau = \frac{Q^2}{4m_p^2}, \quad \epsilon^{-1} = 1 + 2(2 + \tau) \tan^2 \frac{\theta}{2},$$

thus allowing the form factors to be measured in experiments.

Aside: radius from spectroscopy

Spectroscopy is also sensitive to the proton r_E .

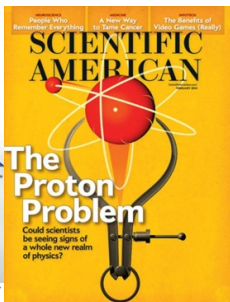
In a hydrogen atom, the S orbitals have the proton located at an antinode of the electron's wavefunction, whereas the P orbitals have it located at a node.



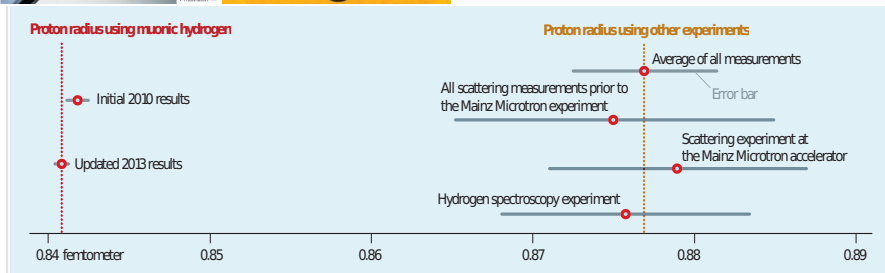
Thus the 2S–2P Lamb shift is sensitive to the finite radius of the proton.

If the electron is replaced by a muon ($200\times$ heavier), the orbitals will be smaller and the effect becomes bigger (2% of the Lamb shift).

Aside: proton radius problem



7σ discrepancy between results from Lamb shift and muonic hydrogen and combined results from electron-proton scattering+spectroscopy.



SOURCE: RANDOLPH

(J. C. Bernauer and R. Pohl, Scientific American, February 2014)

Flavour separation

Form factors of a neutron are measured in experiments using scattering of ^2H or ^3He targets. Using approximate *charge symmetry*, which says that:

- ▶ a u quark in a proton (uud) behaves like a d quark in a neutron (ddu)
- ▶ a d quark in a proton (uud) behaves like a u quark in a neutron (ddu)

then we have

$$G_{E,M}^{Y(p)} = \frac{2}{3}G_{E,M}^u - \frac{1}{3}G_{E,M}^d + \dots$$

$$G_{E,M}^{Y(n)} = \frac{2}{3}G_{E,M}^d - \frac{1}{3}G_{E,M}^u + \dots$$

Neglecting heavier quarks allows the u and d form factors to be isolated.

Measuring strange form factors

Using a single probe (photons) and two targets (protons and neutrons) allows for isolating two flavour contributions.

To isolate the next-largest contribution, from s quarks, use a different probe: Z bosons.

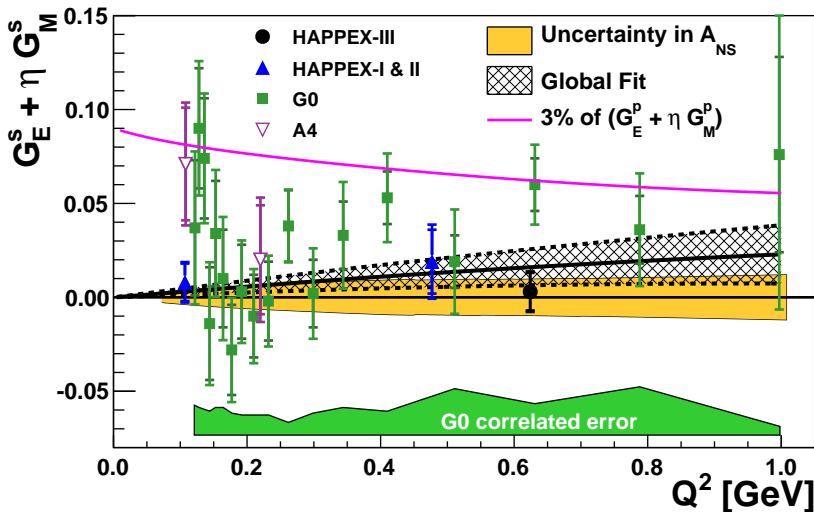
$$J_{\mu}^{ZV} = (1 - \frac{8}{3} \sin^2 \theta_W) \bar{u} \gamma_{\mu} u - (1 - \frac{4}{3} \sin^2 \theta_W) (\bar{d} \gamma_{\mu} d + \bar{s} \gamma_{\mu} s) + \dots$$

By measuring the parity-violating asymmetry in elastic $\vec{e}p$ scattering,

$$A_{LR} = \frac{\sigma_R - \sigma_L}{\sigma_R + \sigma_L},$$

the leading single-photon-exchange contribution can be eliminated and the interference between γ and Z exchange diagrams can be isolated.

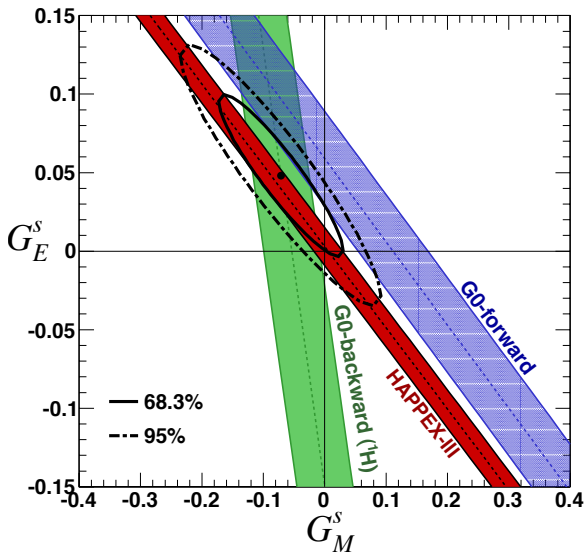
Experiments at forward scattering angles



$$\eta \approx A Q^2, A = 0.94 \text{ GeV}^{-2}$$

(HAPPEX Collaboration, Phys. Rev. Lett. **108** (2012) 102001 [1107.0913])

G_E^s and G_M^s at $Q^2 \approx 0.62 \text{ GeV}^2$



(HAPPEX Collaboration, Phys. Rev. Lett. **108** (2012) 102001 [1107.0913])

... is a regularization of Euclidean-space QCD such that the path integral can be done fully non-perturbatively

- ▶ Euclidean spacetime becomes a periodic hypercubic lattice, with spacing a and box size $L_s^3 \times L_t$.
- ▶ Path integral over fermion degrees of freedom is done analytically, for each gauge configuration. Solving the Dirac equation with a fixed source yields a source-to-all quark propagator.
- ▶ Path integral over gauge degrees of freedom is done numerically using Monte Carlo methods to generate an *ensemble of gauge configurations*.

The $a \rightarrow 0$ and $L_s, L_t \rightarrow \infty$ extrapolations need to be taken by using multiple ensembles.

Nucleon matrix elements using lattice QCD

To find matrix elements, compute

$$C_{2\text{pt}}(t, \vec{p}) = \sum_{\vec{x}} e^{-i\vec{p}\cdot\vec{x}} \langle N(\vec{x}, t) \bar{N}(\vec{0}, 0) \rangle$$
$$\xrightarrow{t \rightarrow \infty} e^{-E(\vec{p})t} |\langle p | \bar{N} | \Omega \rangle|^2$$

$$C_{3\text{pt}}(T, \tau; \vec{p}, \vec{p}') = \sum_{\vec{x}, \vec{y}} e^{-i\vec{p}'\cdot\vec{x}} e^{i(\vec{p}' - \vec{p})\cdot\vec{y}} \langle N(\vec{x}, T) O(\vec{y}, \tau) \bar{N}(\vec{0}, 0) \rangle$$
$$\xrightarrow{\substack{T \rightarrow \infty \\ T - \tau \rightarrow \infty}} e^{-E(\vec{p}')(T - \tau)} e^{-E(\vec{p})\tau} \langle \Omega | N | p' \rangle \langle p' | O | p \rangle \langle p | \bar{N} | \Omega \rangle$$

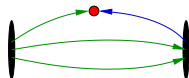
Then form ratios to isolate $\langle p' | O | p \rangle$.

For O a quark bilinear, there are two kinds of quark contractions for $C_{3\text{pt}}$:



Connected contractions

We have efficient solvers for source-to-all quark propagators. Connected contractions can be computed using these via the *sequential propagator* technique.

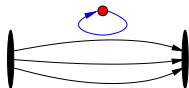


1. Fix the source and compute the **forward** propagator.
2. Fix the sink and T ; compute the **backward** (sequential) propagator.
3. Combine the two to compute arbitrary $O = \bar{q} \dots q$, for all $\tau \in [0, T]$.

For the proton, these contribute for $q \in \{u, d\}$. If we take isovector ($u - d$) observables, then these are the only contributing contractions.

Disconnected contractions

For strange quarks in the proton, these are the only contribution.
Disconnected light quarks are also needed for, e.g., the proton radius.



Using, e.g., $O = \bar{q}\Gamma q$, these involve the **disconnected loop**,

$$T(\vec{q}, t, \Gamma) = - \sum_{\vec{x}} e^{i\vec{q}\cdot\vec{x}} \text{Tr}[\Gamma D^{-1}(x, x)],$$

which involves the quark propagator $D^{-1}(x, y)$ from every point on a timeslice back to itself.

We can estimate the all-to-all propagator stochastically using noise sources η that satisfy $E(\eta\eta^\dagger) = I$. By solving $\psi = D^{-1}\eta$, we get

$$D^{-1}(x, y) = E(\psi(x)\eta^\dagger(y)).$$

Dilution

For a random vector η with components of magnitude $|\eta_i| = 1$, the diagonal of $\eta\eta^\dagger$ is exact and the variance comes from the off-diagonal parts.

$$\text{e.g. } \eta = \begin{pmatrix} \eta_1 \\ \eta_2 \\ \eta_3 \\ \eta_4 \end{pmatrix}, \quad \eta\eta^\dagger = \begin{pmatrix} 1 & \eta_1\eta_2^* & \eta_1\eta_3^* & \eta_1\eta_4^* \\ \eta_2\eta_1^* & 1 & \eta_2\eta_3^* & \eta_2\eta_4^* \\ \eta_3\eta_1^* & \eta_3\eta_2^* & 1 & \eta_3\eta_4^* \\ \eta_4\eta_1^* & \eta_4\eta_2^* & \eta_4\eta_3^* & 1 \end{pmatrix}, \quad E(\eta\eta^\dagger) = I$$

Dilution: use a complete set of projectors $\{P_b | P_b^2 = P_b, \sum_b P_b = I\}$ to partition the components of η and eliminate parts of the variance:

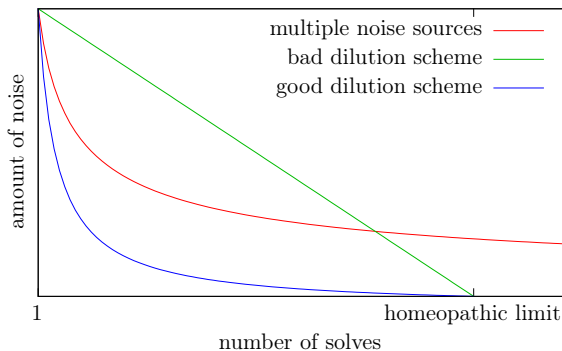
$$\eta^{(b)} \equiv P_b \eta; \quad E\left(\sum_b \eta^{(b)} \eta^{(b)\dagger}\right) = I$$

$$\text{e.g. } \eta^{(1)} = \begin{pmatrix} \eta_1 \\ \eta_2 \\ 0 \\ 0 \end{pmatrix}, \quad \eta^{(2)} = \begin{pmatrix} 0 \\ 0 \\ \eta_3 \\ \eta_4 \end{pmatrix}, \quad \sum_b \eta^{(b)} \eta^{(b)\dagger} = \begin{pmatrix} 1 & \eta_1\eta_2^* & 0 & 0 \\ \eta_2\eta_1^* & 1 & 0 & 0 \\ 0 & 0 & 1 & \eta_3\eta_4^* \\ 0 & 0 & \eta_4\eta_3^* & 1 \end{pmatrix}$$

Dilution

In many cases, using N dilution projectors to target the most important parts of the noise yields a better than $1/\sqrt{N}$ reduction. Commonly used:

- ▶ Spin dilution
- ▶ Colour dilution
- ▶ Spatial dilution



In the *homeopathic limit*, complete dilution is equivalent to fully computing a disconnected loop without stochastic estimation.

Hadamard vectors

Hadamard vectors h_b can be used to obtain the same results as dilution, by taking the component-wise product $\eta^{[b]} \equiv h_b \odot \eta$ and averaging over b .
e.g. Hadamard vectors: $h_1 = (1, 1, 1, 1)$, $h_2 = (1, 1, -1, -1)$

$$\eta^{[1]} = \begin{pmatrix} \eta_1 \\ \eta_2 \\ \eta_3 \\ \eta_4 \end{pmatrix}, \eta^{[2]} = \begin{pmatrix} \eta_1 \\ \eta_2 \\ -\eta_3 \\ -\eta_4 \end{pmatrix}, \quad \frac{1}{2} \sum_b \eta^{[b]} \eta^{[b]\dagger} = \begin{pmatrix} 1 & \eta_1 \eta_2^* & 0 & 0 \\ \eta_2 \eta_1^* & 1 & 0 & 0 \\ 0 & 0 & 1 & \eta_3 \eta_4^* \\ 0 & 0 & \eta_4 \eta_3^* & 1 \end{pmatrix}$$

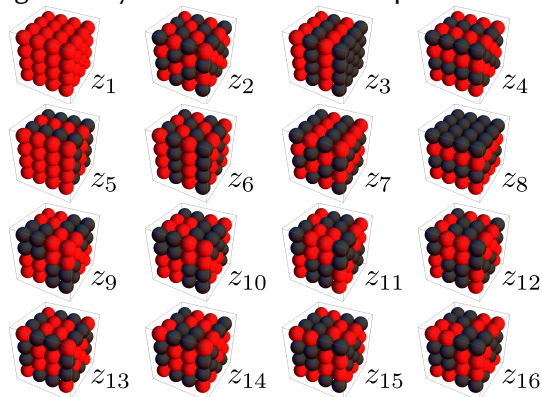
If we had used only $\eta^{[1]}$, we would also get the correct expectation value (only with more noise).

→ Hadamard vectors allow for progressively increasing the level of dilution, while making use of previous effort.

Hierarchical probing

(A. Stathopoulos, J. Laeuchli, K. Orginos, SIAM J. Sci. Comput. **35**(5) (2013) S299–S322 [1302.4018])

Use a sequence of specially-constructed spatial Hadamard vectors in order to progressively increase the level of spatial dilution.



red: +1
black: -1

We use 128 three-dimensional Hadamard vectors to eliminate the variance from neighboring sites up to distance 4.

PHYSICAL REVIEW D **92**, 031501(R) (2015)

High-precision calculation of the strange nucleon electromagnetic form factors

Jeremy Green,^{1,*} Stefan Meinel,^{2,3,†} Michael Engelhardt,⁴ Stefan Krieg,^{5,6} Jesse Laeuchli,⁷
John Negele,⁸ Kostas Orginos,^{9,10} Andrew Pochinsky,⁸ and Sergey Syritsyn³

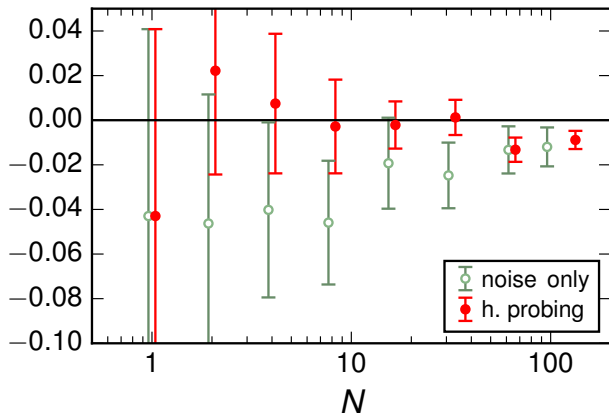
[arXiv: 1505.01803]

- ▶ $N_f = 2 + 1$ Wilson-clover fermions
- ▶ $a = 0.114$ fm, $32^3 \times 96$
- ▶ $m_u = m_d > m_{ud}^{\text{phys}}$, corresponding to pion mass 317 MeV
- ▶ $m_s \approx m_s^{\text{phys}}$
- ▶ 1028 gauge configurations
- ▶ disconnected loops for six source timeslices
(128 Hadamard vectors, plus color+spin dilution)
- ▶ two-point correlators from 96 source positions

Hierarchical probing vs. many noise sources

Study using 1/3 of gauge configurations.

$$G_M^{(\frac{2}{3}u - \frac{1}{3}d)} (Q^2 \approx 0.11 \text{ GeV}^2) \quad (\text{disconnected})$$

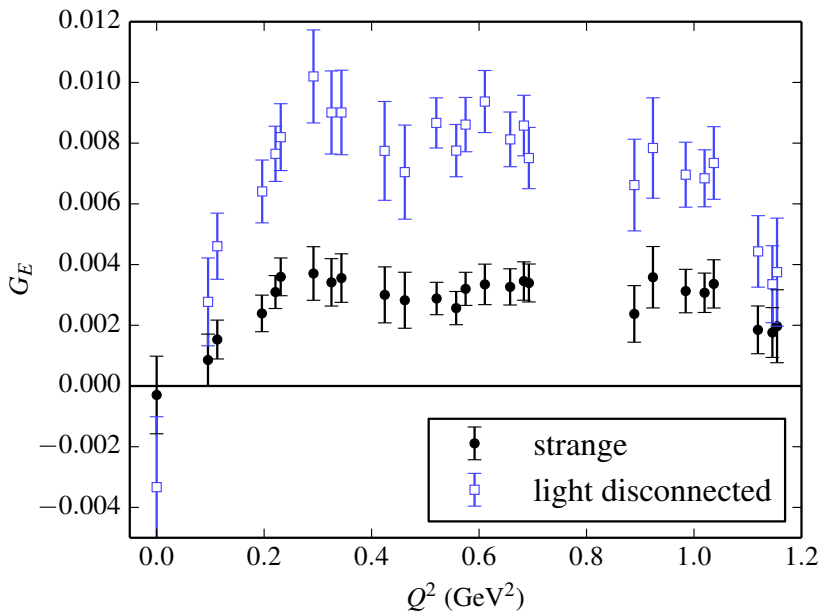


Equal cost at same N
(= N_{Hadamard} or N_{noise}).

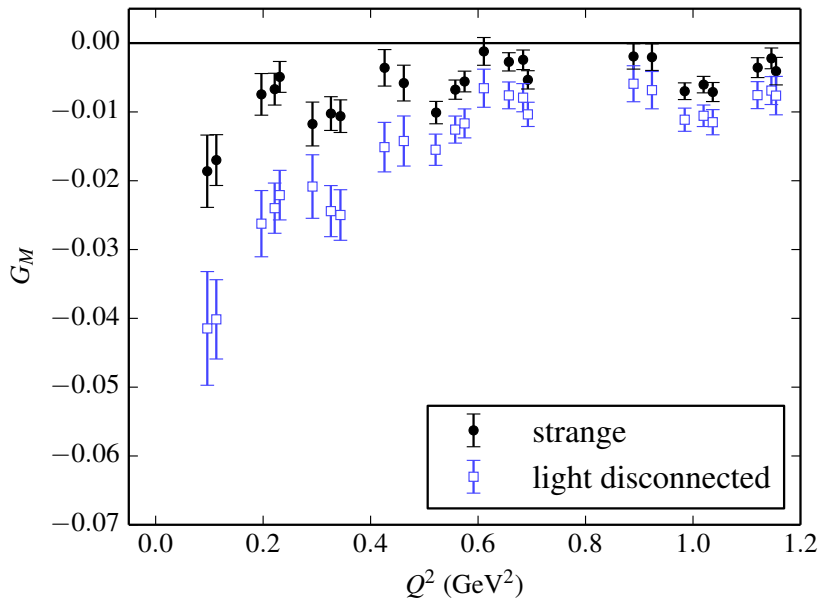
Points offset
horizontally.

(S. Meinel, Lattice 2014)

Disconnected $G_E(Q^2)$



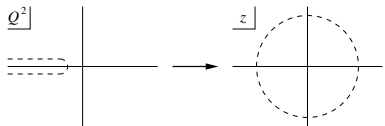
Disconnected $G_M(Q^2)$



Fitting Q^2 -dependence

We want to fit $G_{E,M}(Q^2)$ with curves to determine the radii and magnetic moment from the slope and intercept at $Q^2 = 0$.

- ▶ Common approach: use simple fit forms such as a dipole.
- ▶ Better: use z -expansion. Conformally map domain where $G(Q^2)$ is analytic in complex Q^2 to $|z| < 1$, then use a Taylor series:



[R. J. Hill and G. Paz, Phys. Rev. D **82** (2010) 113005]

$$z(Q^2) = \frac{\sqrt{t_{\text{cut}} + Q^2} - \sqrt{t_{\text{cut}}}}{\sqrt{t_{\text{cut}} + Q^2} + \sqrt{t_{\text{cut}}}},$$
$$G(Q^2) = \sum_k a_k z(Q^2)^k,$$

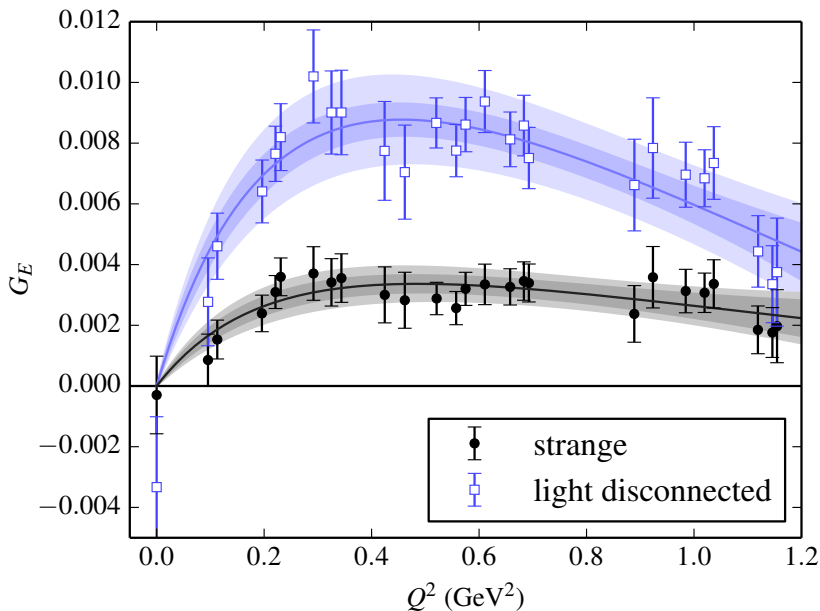
with Gaussian priors imposed on the coefficients a_k . Specifically,

- ▶ For G_E , set $a_0 = 0$ (charge conservation) and leave a_1 unconstrained.
- ▶ For G_M , leave a_0 and a_1 unconstrained.

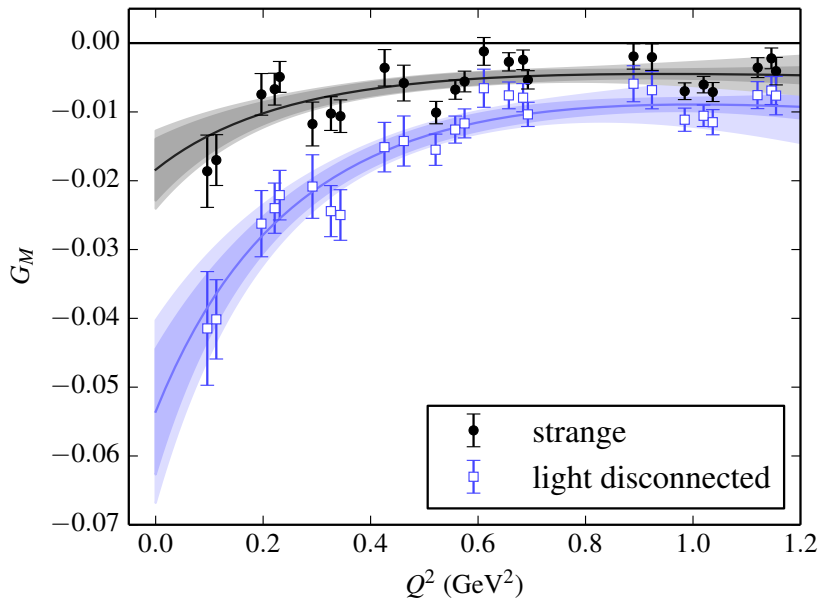
Thus $r_{E,M}$ and μ are not directly constrained.

For higher coefficients, impose $|a_{k>1}| < 5 \max\{|a_0|, |a_1|\}$, and vary the bound to estimate systematic uncertainty.

Disconnected $G_E(Q^2)$



Disconnected $G_M(Q^2)$



Strange magnetic moment and radii at $m_\pi = 317$ MeV

For the unphysical quark masses used on this ensemble:

$$\begin{aligned}(r_E^2)^s &= -0.0054(9)(6)(11)(2) \text{ fm}^2, \\(r_M^2)^s &= -0.0147(61)(28)(34)(5) \text{ fm}^2, \\ \mu^s &= -0.0184(45)(12)(32)(1) \mu_N^{\text{lat}},\end{aligned}$$

where the uncertainties are

1. statistical
2. fitting
3. excited states
4. discretization

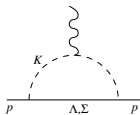
Finite-volume effects neglected since $m_\pi L = 5.9$.

Extrapolation to the physical point

Standard tool used to extrapolate from unphysical quark masses: chiral perturbation theory (ChPT). This is the low-energy effective theory that is an expansion around the $m_q = 0$, $p^2 = 0$ point. For u , d , and s quarks, and nucleons, we need $SU(3)$ heavy baryon ChPT.

- ▶ degrees of freedom: meson octet (π , K , η) and baryon octet (N , Σ , Λ , Ξ)
- ▶ known parameters: meson decay constant f , baryon axial couplings F , D

At leading one-loop order:



$$(r_E^2)^s = \frac{1}{16\pi^2 f^2} \left(c_1(\mu) + \frac{9+5c_{DF}}{3} \log \frac{m_K}{\mu} \right),$$

$$\mu^s = c_2 + \frac{m_p m_K}{24\pi f^2} c_{DF},$$

$$(r_M^2)^s = -\frac{m_p}{48\pi f^2 m_K} c_{DF},$$

where $c_1(\mu)$ and c_2 are unknown parameters, and $c_{DF} = 5D^2 - 6DF + 9F^2$.

Disconnected light-quark observables in ChPT

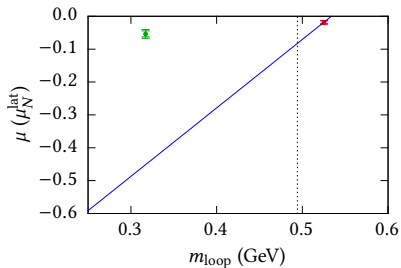
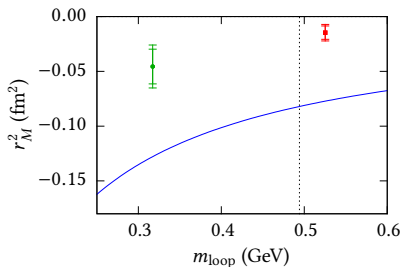
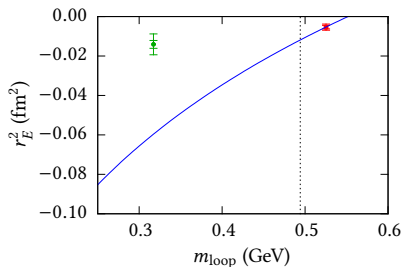
By themselves, the disconnected light-quark form factors are unphysical, but they can be understood in partially quenched QCD and partially quenched ChPT: $q \in \{u, d, s\} \rightarrow q \in \{u, d, s, l, \tilde{l}\}$.

At leading one-loop order, one can simply modify the mass of the strange quark in the loop, i.e., replace m_K with m_{loop} , where

$$m_{\text{loop}} = \begin{cases} m_K & \text{for strange quarks} \\ m_\pi & \text{for disconnected light quarks} \end{cases}$$

Thus with the leading one-loop formulas we can interpolate to the physical kaon mass.

Partially quenched ChPT at leading one-loop order



At this order, PQChPT poorly describes the data.

→ use simple linear interpolation in m_{loop}^2 .

Strange magnetic moment and radii at physical point

Best estimate at physical quark masses: use linear interpolation in m_{loop}^2 :

$$(r_E^2)^s = -0.0067(10)(17)(15) \text{ fm}^2,$$

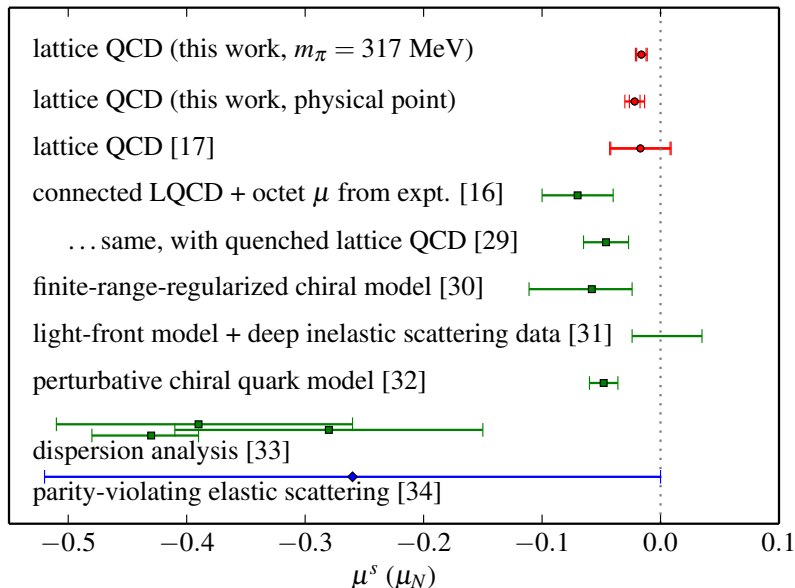
$$(r_M^2)^s = -0.018(6)(5)(5) \text{ fm}^2,$$

$$\mu^s = -0.022(4)(4)(6) \mu_N,$$

where the uncertainties are

1. statistical
2. previously estimated systematics
3. physical-point extrapolation
(= magnitude of shift from result at $m_\pi = 317 \text{ MeV}$)

Strange magnetic moment



Contributions to proton electromagnetic observables

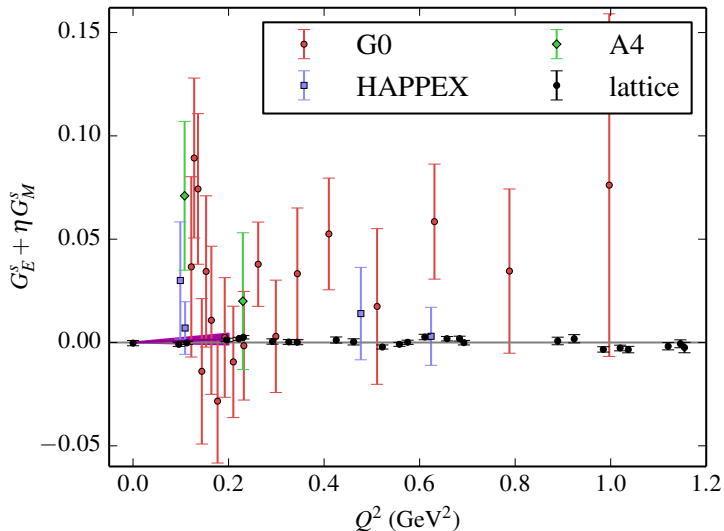
$$(r_E^2)^p = (u, d \text{ contributions}) - \frac{1}{3}(r_E^2)^s \approx (0.88 \text{ fm})^2$$

$$\mu^p = (u, d \text{ contributions}) - \frac{1}{3}\mu^s = 2.793 \dots$$

$$\mu^p (r_M^2)^p = (u, d \text{ contributions}) - \frac{1}{3}(r_M^2)^s \approx 2.793(0.85 \text{ fm})^2$$

In all three cases, the strange-quark contribution is $\sim 0.3\text{--}0.4\%$.

Forward-angle scattering experiments



$$\eta \approx A Q^2, A = 0.94 \text{ GeV}^{-2}$$

Conclusions and outlook

- ▶ High statistics and hierarchical probing methods are effective at producing a signal for the disconnected electromagnetic form factors.
- ▶ Strange quarks contribute a very small amount to the proton radii and magnetic moment ($\sim 0.3\%$).
- ▶ Obtaining a clear nonzero strange-quark signal will be a significant challenge for future parity-violating elastic scattering experiments, especially at forward scattering angles.
- ▶ Additional calculations, especially closer to physical quark masses, are needed to confirm the physical-point estimates.